Molecular Phylogenetics and Evolution 175 (2022) 107560

Contents lists available at ScienceDirect

Molecular Phylogenetics and Evolution

journal homepage: www.elsevier.com/locate/ympev

Recent speciation and phenotypic plasticity within a parthenogenetic lineage of levantine whip spiders (Chelicerata: Amblypygi: Charinidae)

Caitlin M. Baker [a], Jesús A. Ballesteros [b], Shlomi Aharon [c,d], Guilherme Gainett [a], Igor Armiach Steinpress [c,d], Gil Wizen [e], Prashant P. Sharma [a], Efrat Gavish-Regev [c,*]

[a] Department of Integrative Biology, University of Madison-Wisconsin, Madison, WI 53706, United States
[b] Department of Biology, Kean University, Union, NJ 07083, United States
[c] The National Natural History Collections, The Hebrew University of Jerusalem, Edmond J. Safra Campus, Givat Ram, Jerusalem 9190401, Israel
[d] Department of Ecology, Evolution & Behavior, Edmond J. Safra Campus, Givat Ram, Jerusalem 9190401, Israel
[e] 602-52 Park St. E, Mississauga, Ontario L5G 1M1, Canada

ARTICLE INFO

Keywords:
Genotyping-by-sequencing
Molecular clock
Population genomics
Sarax
Sympatry
Troglophile

ABSTRACT

Caves constitute ideal study systems for investigating adaptation and speciation, as the abiotic conditions shared by aphotic habitats exert a set of environmental filters on their communities. Arachnids constitute an important component of many cave ecosystems worldwide. We investigated the population genomics of two whip spider species: *Sarax ioanniticus*, a widely distributed parthenogenetic species found across the eastern Mediterranean; and *S. israelensis*, a recently described troglomorphic species that is endemic to caves in Israel. Here, we show that *S. israelensis* is completely genetically distinct from *S. ioanniticus* and most likely also a parthenogen. Counterintuitively, despite the lack of genetic variability within *S. ioanniticus* and *S. israelensis*, we discovered considerable variation in the degree of median eye reduction, particularly in the latter species. Natural history data from captive-bred specimens of *S. israelensis* validated the interpretation of parthenogenesis. Our results are most consistent with a scenario of a sexual ancestral species that underwent speciation, followed by independent transitions to apomictic parthenogenesis in each of the two daughter species. Moreover, the lack of genetic variability suggests that variation in eye morphology in *S. israelensis* is driven exclusively by epigenetic mechanisms.

1. Introduction

Subterranean habitats exist globally and include both artificial and natural cavities. Although natural cavities (e.g., caves) can be formed by various mechanisms (e.g. volcanic, glacial, mechanical and erosion/solution processes) in different climates, rock formations, and biogeographical regions, most of them share abiotic characteristics, such as limitation of light, stable and narrow ranges of temperatures, and often high relative humidity (Howarth, 1993, 1983, 1980; Howarth and Moldovan, 2018; Mammola, 2019; Poulson and White, 1969). The communities of these habitats are strongly shaped by environmental filtering and can include species with different levels of affinities and adaptations to the subterranean habitats.

It is well established that life in aphotic conditions leads to atrophy of structures that are not in use, while selection acts positively on other structures that will give advantage in the hypogean habitat (Barr and Holsinger, 1985; Protas and Jeffery, 2012). Indeed, many cave-dwelling animals around the world are troglomorphic and present special morphological, behavioral, and physiological features that are associated with life in darkness. The most salient of these are the reduction or complete loss of eyes, depigmentation, lowered metabolic activity, and compensatory gains in tactile and/or olfactory capacity; many of these adaptations have been shown to have a strong underlying genetic basis (Protas et al., 2011, 2006; Re et al., 2018; Riddle et al., 2018). The extent of troglomorphism is generally thought to be correlated with duration of isolation in cave habitats, although a body of work on the population genetics of Mexican cavefish (*Astyanax mexicanus* (De Filippi, 1853)) has shown that adaptations like eye and pigment loss can occur repeatedly, on short time scales, and in the face of gene flow (Bradic et al., 2013, 2012; Moran et al., 2022). These considerations influence the recognition and delimitation of cave-adapted species and have downstream consequences for assessments of conservation priority.

* Corresponding author.
E-mail address: efrat.gavish-regev@mail.huji.ac.il (E. Gavish-Regev).

https://doi.org/10.1016/j.ympev.2022.107560
Received 21 March 2022; Received in revised form 25 May 2022; Accepted 2 June 2022
Available online 30 June 2022

Within arachnids, several groups are known to be associated with caves, and troglobitic arachnid lineages account for key components of cave ecosystems worldwide (Mammola et al., 2018a, 2018b, 2018c; Mammola and Isaia, 2017). One such group is the order Amblypygi (commonly, "whip spiders" or "tailless whip scorpions"), which are notable for their unusual appearance and their characteristic antenniform first pair of walking legs (the "whips"). Most of the species of this order constitute short-range endemics, making the lineage significant for studies of historical biogeography (Esposito et al., 2015; Miranda et al., 2021a, 2021b). One exception to this trend is *Sarax ioanniticus* (Kritscher, 1959) (family Charinidae Quintero, 1986, transferred from the genus *Charinus* Simon, 1892 by Miranda et al. (2021a), a parthenogenetic and synanthropic species that is broadly distributed in the Eastern Mediterranean region (Egypt, Greece, Israel, Italy, Jordan, Syria, and Turkey; Fig. 1) (Agapakis and Miranda, 2019; Colla et al., 2020; Miranda et al., 2016; Shakhatreh et al., 2020; Weygoldt, 2007). In 2016 a troglomorphic congener, *Sarax israelensis* (Miranda, Aharon, Gavish-Regev, Giupponi and Wizen, 2016), was discovered from two localities in Israel. This species is readily distinguished from *S. ioanniticus* by its reduced median and lateral eyes, smaller size, fewer pedipalpal spines, and wider carapace shape (Miranda et al., 2016). However, both species exhibit a loose association with caves, and both can be found in cool, humid environments, including human-made structures (e.g., cisterns, sewers, and walls of old buildings). Intriguingly, as with *S. ioanniticus*, only females are known from *S. israelensis*, leading to the suggestion that this species may likewise be parthenogenetic (Miranda et al., 2016).

A recent phylogeny of the family Charinidae based on combined analysis of morphological and molecular data showed that *S. ioanniticus* and *S. israelensis* constitute sister species (Miranda et al., 2021b). However, due to the absence of molecular sequence data for *S. israelensis*, neither the timing of the pair's split nor the mechanism of speciation could be inferred. The only other molecular resources for this pair are developmental transcriptomes of both species that were recently generated to investigate the developmental genetic basis for eye loss in arachnids. These datasets were used to pinpoint arachnid-specific candidate genes for eye development, culminating in the identification of the transcription factor paralog *sine oculis-A* as a central player in both median and lateral eye morphogenesis in arachnids (Gainett et al., 2020).

To determine whether *Sarax israelensis* constitutes a distinct genetic species from *S. ioanniticus*, as well as to investigate the geographic structure of *Sarax* Simon, 1892 populations within Israel, we inferred population-level relationships using genome-skimming and barcoding approaches. In addition, we assessed the degree of eye reduction and/or loss across the range of *S. israelensis* to establish the strictness of its diagnosis. Here, we show that the two species are distinct lineages and exhibit no evidence of gene flow. Nevertheless, we found a high degree of polymorphism in eye condition, particularly within *S. israelensis*. Given that *S. israelensis* appears to be a parthenogenetic species, our results suggest that the degree of arachnid eye reduction may be a more plastic trait in natural populations that previously appreciated.

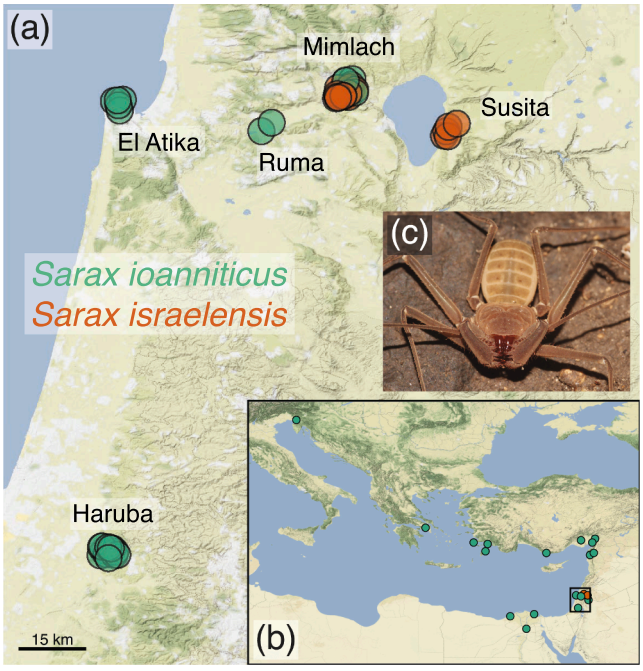

Fig. 1. Map of the distribution of *Sarax ioanniticus* and *S. israelensis*. (a) Localities of Israeli *Sarax* samples used in this study, where each point depicts one individual sampled in this study. (b) Locator map of the eastern Mediterranean, with each point corresponding to all known localities of both *Sarax* species. Black rectangle outlines the region shown in (a). (c) Live habitus of *S. israelensis*. Photo by S. Aharon.

2. Materials and methods

2.1. Field sampling and phenotypic variation

A total of 45 *Sarax* individuals were collected from five caves in northern and central Israel in July–August 2018 and May 2021 (Supplementary Table S1; Fig. 1). Out of more than 100 additional caves (natural and human-made) explored across Israel, to date *Sarax* has only been found to inhabit these five localities. Taxonomic identification of adults was performed using light microscopy (primarily looking at eye morphology), following the descriptions of Miranda et al. (2016).

To document eye condition, photographs were taken of the carapace in dorsal aspect on a Leica MC120 HD camera mounted on a Leica M60 stereomicroscope, driven by Leica Application Suite v.4.8. A single image was captured per specimen.

2.2. Construction and analysis of a barcoding dataset

To determine the relationships of Israeli *Sarax* to each other as well as other congeners outside the Levant, we sequenced the mitochondrial locus cytochrome *c* oxidase subunit I (hereafter, COI) for a subset of 12 individuals (out of 45 available), representing all five localities and both morphospecies.

2.2.1. Sequencing and analysis of COI locus

COI was amplified using the primers LCO and HCOout using 2 ul of template DNA, 35 cycles of polymerase chain reaction (PCR), and an annealing temperature of 50 °C. Amplification products were verified by gel electrophoresis and purified using the GeneJET PCR Purification Kit (Thermofisher). The purified products were then sent for DNA sequencing (EZ-Seq, Macrogen, USA). Additionally, we downloaded from GenBank the published COI sequences of two samples of *S. ioanniticus* (MT040909, from Greece; MT040910, from Turkey); two samples of *S. seychellarum* (MT040927, MT040928), the phylogenetically closest species for which molecular data exist (the "West Asia clade" of *Sarax*, *sensu* Miranda et al. (2021b)); and two samples of *S. rimosus* (MT040923, MT040924), a species from the "East Asia clade" of *Sarax* as the outgroup. Newly sequenced COI sequences for this study are deposited in GenBank (accession numbers ON303815–ON303826).

COI sequences were aligned using MAFFT v.7 (Katoh and Standley, 2013) using default parameters and automatic algorithm selection (-auto). The resulting alignment was then trimmed using GBlocks v.0.91b (Castresana, 2000) to remove end regions until at least 15 sequences were represented. We also used DAMBE7 (Xia, 2018) to assess substitution saturation levels in each codon position of COI. Finally, a phylogenetic tree was inferred from the alignment using IQ-TREE v.1.6 (Nguyen et al., 2015), implementing automatic substitution model

selection in ModelFinder (Kalyaanamoorthy et al., 2017) and assessing nodal support with Shimodaira-Hasegawa approximate likelihood ratio resting (SH-aLRT) and ultrafast bootstrap resampling (UFBoot) (Hoang et al., 2018). Each measure of nodal support implemented 1000 bootstrap resampling replicates.

2.2.2. Divergence time estimation

We used an iterative strategy to identify the best clock model and tree prior for our COI dataset using the Path sampler application in BEAST v.2.4 (Bouckaert et al., 2014). First, we launched three path sampling analyses all under a Yule tree prior with 100 steps of 1 million generations, corresponding to a strict clock, an exponential relaxed clock, and a lognormal relaxed clock. Marginal likelihood estimates were compared using Bayes Factors to select the best clock model. We then launched another path sampling analysis under the best clock model but varying the tree prior. We tested birth–death and fossilized birth–death models against the Yule model, and again compared the marginal likelihood estimates using Bayes Factors. For all path sampling analyses, we applied the optimal site substitution model identified under the Bayesian Information Criterion (BIC) in ModelFinder (Kalyaanamoorthy et al., 2017).

We estimated lineage ages in BEAST under the best clock model and tree prior. Divergence time estimations were performed using a published substitution rate of COI for spiders (family Dysderidae) (Bidegaray-Batista and Arnedo, 2011). This constitutes the phylogenetically closest comparison available to an amblypygid (both are members of the chelicerate clade Tetrapulmonata). This strategy was used as there are no fossils known from the genus *Sarax*, nor for the family Charinidae more broadly. We set the clock rate prior (ucld.mean) to 0.0199 (lower: 0.0136; upper: 0.027), corresponding to the mean lognormal clock estimate and 95% highest probability density (HPD) from Bidegaray-Batista and Arnedo (2011). We launched two independent runs, each with 100 million generations, and assessed stationarity and convergence in Tracer 1.7 (Rambaut et al., 2018), confirming all ESS values were greater than 200. These were then combined in LogCombiner using a 10% burnin for each run, and TreeAnnotator was used to generate the final maximum clade credibility tree using mean node heights.

2.3. Construction and analysis of a population genomic datasets

To infer dynamics within each species complex using a genome-skimming approach, we sequenced all 45 available specimens of *Sarax*. Specifically, the resulting SNP dataset was used to test for the possibility of gene flow or incomplete lineage sorting.

2.3.1. Genotyping-by-sequencing library preparation, assembly, and matrix construction

Genomic DNA was extracted from two to eight legs from all specimens using the Qiagen DNeasy Blood and Tissue (Qiagen, Valencia, CA) kit with an overnight incubation and final elution in 10 mM Tris-HCl. DNA concentrations were quantified using a Qubit Fluorometer (Life Technologies, Inc) High Sensitivity kit, and quality was assessed using gel electrophoresis. Preparation for genotype-by-sequencing (GBS) libraries was performed at the University of Wisconsin–Madison Biotechnology Center using the restriction enzymes *Nsil* and *Bfal*. Digested samples were individually barcoded using unique dual indexes, pooled, and size selected. Libraries were sequenced on an Illumina NovaSeq 6000 as 150 bp paired-end reads. Raw sequences are deposited in the Sequence Read Archive (SRA) under BioProject PRJNA826492.

Raw DNA sequences were processed in ipyrad v 0.9.68 (Eaton and Overcast, 2020) using paired ddRAD as the datatype and implementing default parameter values for demultiplexing (no barcode mismatches allowed) and filtering (maximum of 5 low quality bases, minimum read length of 35 bp). Within each sample, reads were clustered using a de novo assembly method at the default value of 85% similarity. Estimation of heterozygosity and error rate assumed a diploid genome (*max_alleles_consens* = *2*). Consensus base calling and filtering allowed no more than 5% of bases in a locus to be uncalled as Ns. Sequences were then clustered across samples at a minimum of 85% similarity and aligned using MUSCLE v.5 (Edgar, 2004). Finally, all loci with a minimum of 23 samples (i.e., 50% taxon occupancy) and a maximum of 8 indels were included in the final data matrix and used for subsequent analysis.

2.3.2. Phylogenetic and population genomic analyses of GBS data

We reconstructed phylogenetic relationships of our samples in IQ-TREE v.1.6 using both the loci and the SNP data generated in ipyrad for our 50% occupancy matrix. For the SNP alignment, we implemented the ascertainment bias correction (+ASC) with our substitution model testing. For both analyses, nodal support was assessed using 1000 replications of both SH-aLRT and UFBoot. Given the reciprocal monophyly of *S. ioanniticus* and *S. israelensis* recovered by the COI tree, we rooted the phylogeny between these two clades.

Population genomic analyses were performed on a data matrix consisting of one phased SNP from each locus assembled in ipyrad (.ustr file). We first used the program ParallelStructure (Besnier and Glover, 2013; Pritchard et al., 2000) in the CIPRES Science Gateway to characterize population substructure and identify admixture in the Israeli *Sarax*. We conservatively specified an ancestry model allowing admixture and correlated allele frequencies, following the recommendations of Porras-Hurtado et al. (2013). To determine the optimal number of groups within our samples, we tested values of K = 1–5, using 10 iterations for each K value and 100,000 Markov chain Monte Carlo (MCMC) generations following a burn-in of 50,000 generations. Optimal K value was determined using the delta K method of Evanno et al. (2005), implemented in STRUCTURE HARVESTER (Earl and vonHoldt, 2011), which compares the value of K to the rate of change of the likelihood function, and by visually inspecting the change in *Ln P(D)* for each K value.

We also calculated standard population genetic statistics for both species in the program GenoDive v3.03 (Meirmans and Van Tienderen, 2004), replacing any missing data by randomly drawing alleles based on the overall allele frequencies within each species. We did this for the dataset of all 45 individuals as well as on datasets composed of each species alone. As before, the minimum taxon occupancy for a locus to be included in the final dataset was 50% (i.e., represented in $\geq$ 10 *S. israelensis* samples and $\geq$ 13 *S. ioanniticus* samples). These statistics included number of alleles observed per species (Num), observed (H_o) and expected (H_s) heterozygosity, and inbreeding coefficient (G_{IS}). Population differentiation between the species was calculated (F_{ST}), using 999 permutations to assess significance. Finally, a hierarchical analysis of molecular variance (AMOVA) was performed in GenoDive using an infinite allele model and 999 permutations to assess significance.

2.4. Test of parthenogenesis in S. israelensis

To validate the inference of parthenogenesis in *S. israelensis* (Miranda et al., 2016), natural history data were collected from captive specimens. Twenty live *S. israelensis* were collected through visual searching along the walls and ceiling of two caves in northern Israel (ten individuals from each of the caves, Susita and Mimlach) on several occasions in 2013–2015. Specimens were captured and observed for several years in the laboratory at 24°–26° C in a dark room, and were fed with live silverfish, isopods, and cricket nymphs. Each specimen was kept separately in 10 × 5 × 5 cm acrylic container (AMAC Plastics Ltd., California, USA) with moist peat substrate and a Styrofoam board placed diagonally as a resting spot. To eliminate the possibility of sexual reproduction prior to collection, molting events were recorded, as sperm is not stored by females between molts. After molting, specimens were then inspected for signs of developing oocytes through their opisthosoma, production of eggs, and hatching of praenymphae. The number of

offspring per clutch was also recorded. The captive-bred offspring were kept under the same conditions as the wild-collected specimens, and isolated from other individuals since birth. Upon reaching one year of age, they were inspected on a monthly basis for signs of developing oocytes.

3. Results

3.1. Phenotypic variation and habitat

Of the 20 sampled specimens of *S. israelensis*, eight were blind (lacking median eyes altogether; Fig. 3E) and the rest had reduced median eyes (Fig. 3D, 3F). None of the *S. israelensis* individuals had fully developed median eyes (i.e., comparable to *S. ioanniticus*). Of the 25 sampled *S. ioanniticus*, one had reduced median eyes (Fig. 3C), though these eyes did not exhibit the same degree of reduction as in *S. israelensis*. All other *S. ioanniticus* individuals had fully formed median eyes (Fig. 3B; Supplementary Fig. S1).

Both *Sarax* species were found in dark and humid habitats, mainly manmade ancient water cisterns, spring tunnels and rock-cut caves, but *S. ioanniticus* can also be found in humid rooms of recently constructed dwellings. Mimlach cave, where both species are found, is located eight kilometers west of the Sea of Galilee. It is a typical rock-cut cave and was used as a subterranean hiding complex during the Jewish revolts against the Roman empire (66 –136 CE). The cave is composed of narrow tunnels, carved in the soft chalk of the Cretaceous-aged Menuha Formation (~80 mya). Individuals of both species were collected in Mimlach cave mainly on the lime-plastered walls of a water cistern, which was breached by the excavation of the hiding tunnels during the revolts.

The second locality, where only *S. israelensis* was found, is Susita cave, located at the western slopes of the Golan Heights along the Jordan Rift Valley, two kilometers east of the Sea of Galilee. The cave formed naturally in the Pliocene Cover Basalt Formation (dated to 4.3–5.0 mya; (Segev et al., 2022)), which in turn sits atop the middle Miocene Hordos Formation (13–15 mya). Hordos Formation composed primarily of sedimentary rocks such as conglomerates, limestones, sandstones, siltstones, and mudstones (Mor et al., 1997). During the Hellenistic period (1st–2nd centuries BC), the cave walls were plastered and it was used as a water cistern (Michael Eisenberg, *personal communication*). Eventually, the cave opening collecting running water was closed and the cave was used for other purposes, including storage and industry.

Sarax ioanniticus, the widely distributed amblypygid species, was collected from ancient human-made caves in a variety of rock types and geological formations in Israel, such as Horbat Ruma (lower Galilee),

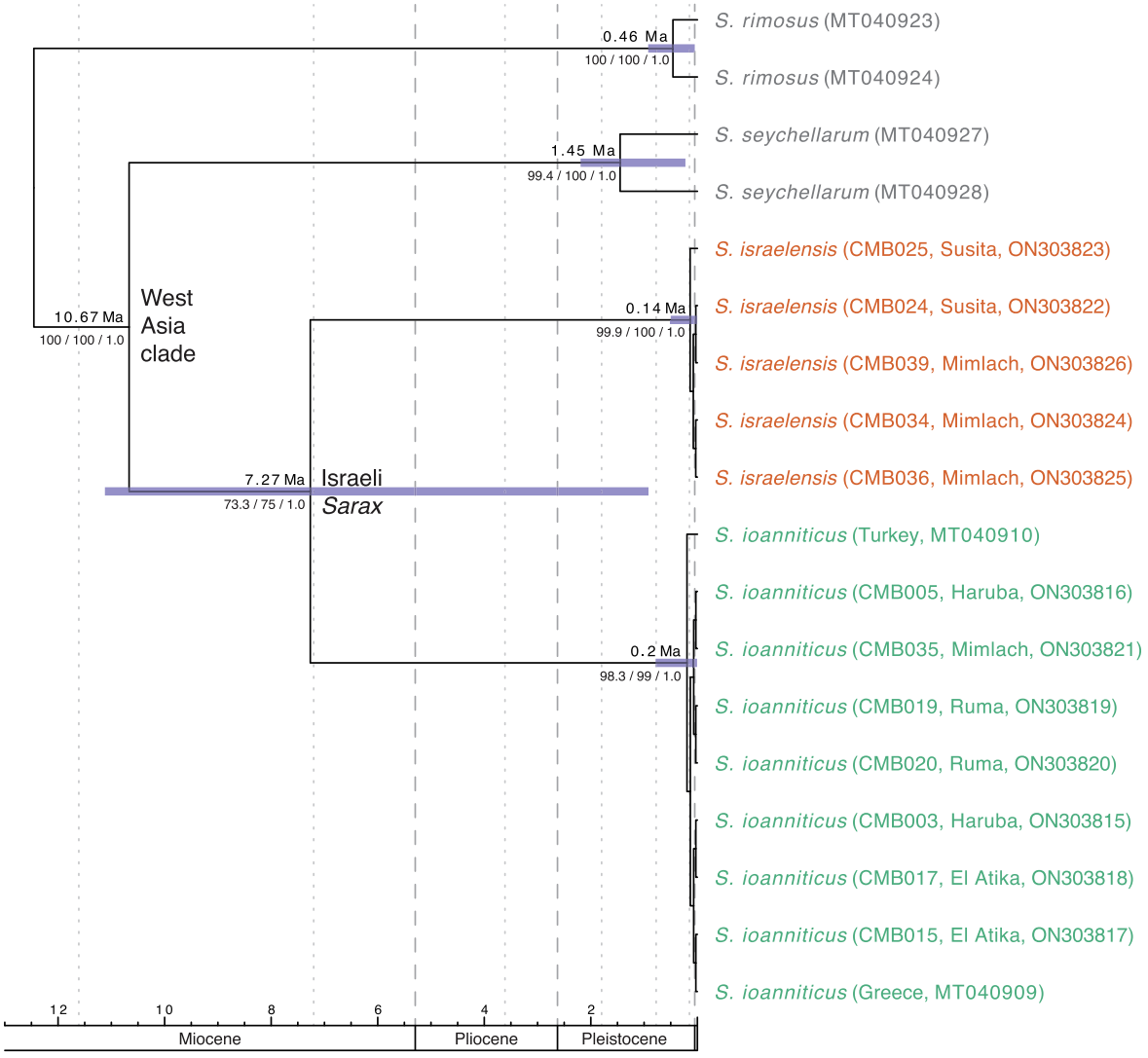

Fig. 2. Chronogram of *Sarax* based on spider COI substitution rate. Estimated divergence times in millions of years (Ma) shown above nodes. Numbers below nodes show SH-aLRT, UFBoot, and BEAST posterior probabilities, in that order. Purple bars at nodes correspond to 95% highest probability densities (HPD). Terminals colored by species, as in Fig. 1. (For interpretation of the references to colour in this figure legend, the reader is referred to the web version of this article.)

Haruba cave (Judean foothills), and even in the geologically young El ‘Atika burial cave, located 250 m from the Mediterranean Sea and excavated in a calcareous sandstone that formed during the Pleistocene (11,000 years ago–1.7 mya).

3.2. COI analysis and divergence dating

A test of substitution saturation in DAMBE found all three codon positions of the COI alignment to be suitable for phylogenetic analysis (Supplementary Table S2). Phylogenetic analysis of COI in IQ-TREE recovered the reciprocal monophyly of the two Israeli *Sarax* species, to the exclusion of *S. seychellarum* (SH-aLRT = 73.3, UFBoot = 75; Supplementary Fig. S3), a result consistent with previous morphological analyses (Miranda et al., 2021b, 2016).

Path sampling analysis and comparison of Bayes Factors found a combination of a lognormal relaxed clock and a birth–death tree prior to be ideal (BF = 12.63 compared to next highest model’s marginal *L* estimate; Supplementary Table S3). Using the dysderid spider COI substitution rate, we found that *S. ioanniticus* and *S. israelensis* split 7.27 mya (95% highest posterior density interval [HPD]: 0.92–11.12 mya). The coalescence times for *S. ioanniticus* and *S. israelensis* were estimated to be 0.14 (0.002–0.5) and 0.02 (0.01–0.78) mya, respectively (Fig. 2). However, due to violations of model assumptions (asexual reproduction; inclusion of multiple individuals within a species), we suspect that the ages of these species are underestimated.

The two exemplars of *S. seychellarum* were estimated to have diverged 1.45 (0.22–2.19) mya. This result does not accord with the divergence dating results of Miranda et al. (2021b), which recovered a divergence between these two individuals 9.87 mya and used five loci and two fossil calibrations to estimate divergence times. Similarly, the Israeli *Sarax* and *S. seychellarum* were recovered as diverging 10.67 (1.38–15.89) mya in our analysis, though in Miranda et al. (2021b) this divergence was estimated to be far older at 139.7 mya. Such markedly different estimates may be the result of an artificially long branch in the analysis of Miranda et al. (2021b), induced by the absence of more closely related taxa such as *S. israelensis* (for which no molecular data existed prior to our study).

3.3. Population genomic datasets

De novo assembly of a 50% occupancy matrix recovered 40,847 loci across the 45 samples, with a mean of 24,599 loci per individual (Supplementary Table S1). This matrix contained 389,427 total SNPs, with 40.5% missing site data.

3.3.1. Phylogenomic analyses using GBS

For the population genomic analyses of both species together, we used a matrix consisting of one SNP per locus generated in ipyrad, totaling 40,632 unlinked SNPs. The genetic diversity analysis of *S. ioanniticus* alone was performed on a 50% occupancy matrix

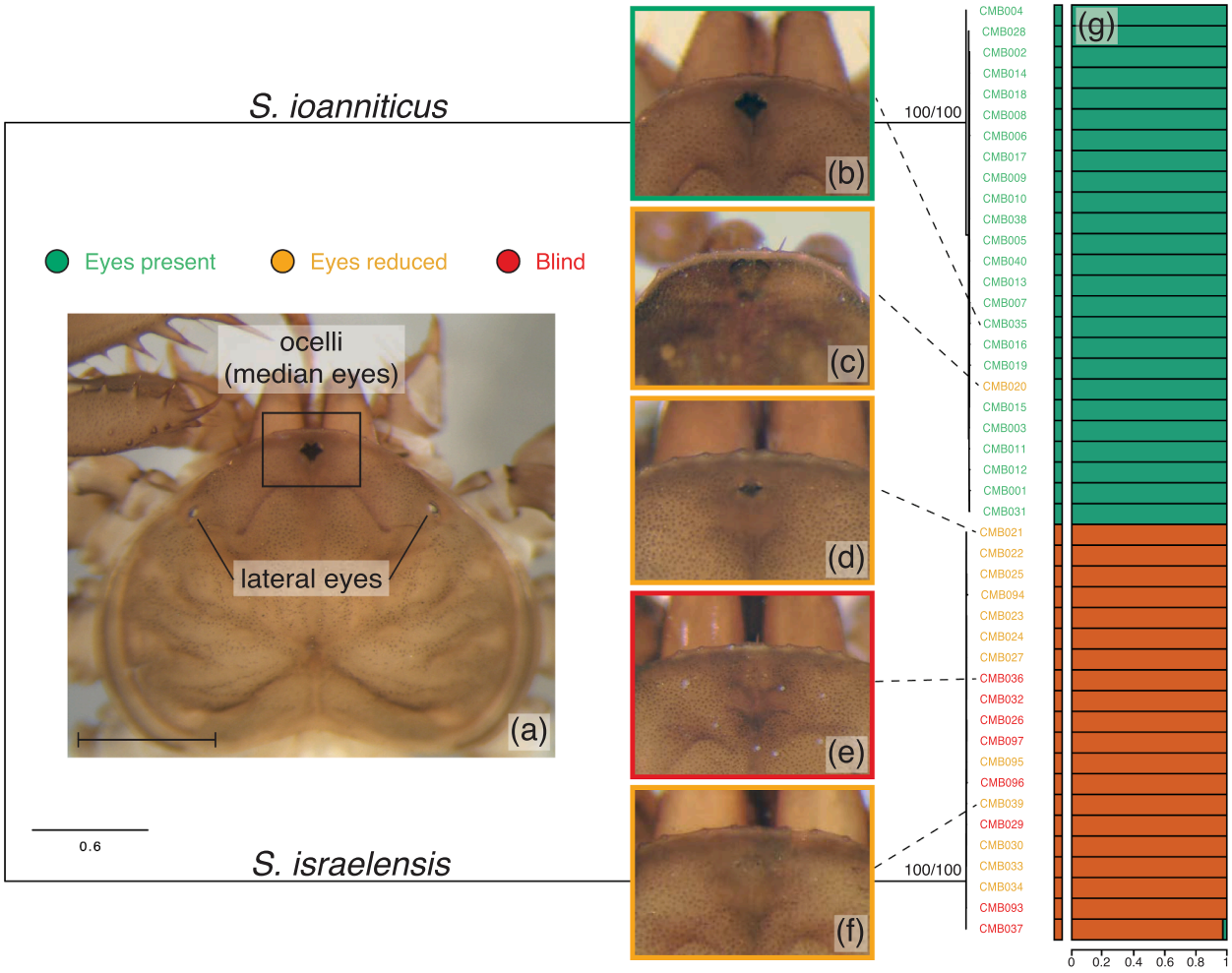

Fig. 3. GBS phylogeny of Israeli *Sarax* based on IQ-TREE analysis of 389,427 SNPs. Numbers at nodes show SH-aLRT and UFBoot values. Terminals colored by eye morphology. (a) Dorsal view of carapace of *S. ioanniticus* (CMB001), showing location of lateral and median eyes. Black rectangle around median eyes corresponds to the region shown in (b–f). Scale bar: 1 mm. (b–f) Exemplars Israeli *Sarax* showcasing the diversity of median eye development. Dotted lines connect image to its respective terminal in the phylogeny. (g) Results of STRUCTURE analysis based on 40,632 unlinked SNPs, where K = 2. Colors correspond to species, as in Figs. 1, 2.

composed of 106,225 unique SNPs across 25 samples (Supplementary Table S4). For *S. israelensis*, our final dataset had 122,952 unlinked SNPs across 20 samples (Supplementary Table S5).

ModelFinder using the ascertainment bias correction and the Bayesian information criterion (BIC) found the best model for phylogenetic reconstruction of all SNPs to be TPM2 + F + R2. The best model for the alignment of concatenated loci was K3Pu + F + R7. For both input datasets, tree reconstruction in IQ-TREE recovered two well-defined and reciprocally monophyletic clades, one corresponding to *S. ioanniticus* and one to *S. israelensis* (Fig. 3, Supplementary Fig. S3). Each clade received full support (100% SH-aLRT and UFBoot). Within each species, branch lengths were close to 0, reflecting minimal genetic diversity within each species. The two species were found to co-occur in a single locality (Mimlach cave; Fig. 1).

3.3.2. Population genomic analyses

Analysis of populations using STRUCTURE and delta K strongly supported the division of the dataset into two clusters, one corresponding to *S. israelensis* and one corresponding to *S. ioanniticus*. Sample assignments into these clusters perfectly recapitulated the phylogenetic tree. Furthermore, we found no evidence of admixture between the different species. At most, the sample CMB037 (*S. israelensis*) showed 2.43% of SNPs associated with *S. ioanniticus* (Fig. 3).

Pairwise genetic differentiation (F_{ST}) between the two species as calculated in GenoDive was extremely high (0.976, *p*-value 0.001). This was corroborated by AMOVA, which also recovered 97.6% of all genetic diversity as being found between the two species. Only 2.4% of the genetic variation corresponded to variation within individuals, and no genetic variation was attributable to variation between individuals of the same species (Table 1). Similarly, when *S. ioanniticus* and *S. israelensis* were analyzed on their own, 99.3% and 99.9% of genetic variation, respectively, was attributable to variation within individuals (Supplementary Tables S6, S7).

We also assessed genetic diversity within each species (Table 2). The observed heterozygosity (H_o, the frequency of heterozygotes within each species) and expected heterozygosity (H_s, expected heterozygosity assuming Hardy-Weinberg equilibrium and corrected for sampling size) for both species was 0.017, supporting the hypothesis that individuals within each species are genetic clones.

3.4. Parthenogenesis in S. israelensis

Of the 20 collected specimens of *S. israelensis*, 11 showed signs of developing oocytes through their opisthosoma after molting (Fig. 4A). Egg clutches were lain ca. one year later (Fig. 4B), and egg development lasted 90 days at 24°–26° C. The number of hatching praenymphae per egg clutch ranged from 9 to 25. In some cases, several eggs in a clutch did not hatch successfully. Many of the protonymphae, the stage that molts from praenymphae and leaves the mother's back, died on the first days after molting, possibly due to starvation. Of the surviving 24 protonymphae, eight individuals started showing signs of developing oocytes and mature ova at the age of five years (Fig. 4C). Rearing data are provided in Table 3.

Table 1
Results of AMOVA based on analysis of all 45 samples and 40,632 unlinked SNPs, as calculated in GenoDive.

Source of variation	Nested in	%var	F-stat	F-value	Std. dev.	p-value
Within individual	—	2.4%	F_{IT}	0.976	0.000	—
Between individuals	Species	0.0%	F_{IS}	−0.003	0.002	0.963
Between species	—	97.6%	F_{ST}	0.976	0.000	0.001

Table 2
Indices of genetic diversity metrics for both species of Israeli *Sarax*. N: number of individuals sampled in each species; Num: number of alleles observed per species; H_o: observed heterozygosity; H_s: expected heterozygosity under equilibrium; G_{IS}: inbreeding coefficient.

	n	Num	H_o	H_s	G_{IS}
S. ioanniticus	25	1.219	0.017	0.017	0.010
S. israelensis	20	1.169	0.017	0.017	−0.020
All species	45	2.006	0.017	0.017	0.011

4. Discussion

The discovery that troglomorphic traits can evolve rapidly within a species despite ongoing gene flow, as exemplified by the cavefish *A. mexicanus*, has challenged the traditional conception of troglobitism as the result of gradual, irreversible changes that culminate as evolutionary dead-ends (Cope, 1896; Dollo, 1893; Gould, 1970; Huxley, 1942; Mayr, 1942; Prendini et al., 2010; Wagner, 1982). While examples abound within arachnids of troglobitic species that represent true evolutionary relicts, the possibility of recent speciation between epigean and hypogean lineages prompts reexamination of traditional paradigms for evolutionary origins of troglomorphism. The present investigation therefore focused on generating molecular sequence data for the recently described troglomorphic species *S. israelensis*, toward testing the phylogenetic position, divergence time, and reciprocal monophyly of this taxon with respect to its congener, *S. ioanniticus*.

Consistent with previous identifications based on morphology (Miranda et al., 2016), molecular analyses unambiguously accord with the delimitation of *S. ioanniticus* and *S. israelensis* as genetically distinct, reciprocally monophyletic species. Despite the relatively recent divergence of the species pair, we found no evidence of incomplete lineage sorting across our dataset, nor evidence of population structure in either species. Even within the geographically widespread *S. ioanniticus*, COI sequence data from specimens collected in Greece and Turkey were genetically identical to specimens collected in Israel.

One of the localities *S. israelensis* inhabits (Susita) is originally a natural basalt cave that formed during or after the deposition of the Pliocene Cover Basalt Formation (4.3–5.0 mya) and was subsequently plastered during the Hellenistic period (1st–2nd centuries BC) by humans. The Cover Basalt Formation sits atop the older Hordos Formation (middle Miocene, 13–15 mya), which was formed from sedimentary deposition in freshwater lake areas and fluvial systems of the continental basin during a warm period. The present day Galilee Sea region, was tectonically isolated from the Mediterranean Sea by the uplifting of the central mountain range of Israel ~ 7 mya (Matmon et al., 2003). These geological and historical data may be related to the diversification of *Sarax* in Israel, however our estimate for the Israeli *Sarax* divergence, ca. 7.27 mya (HPD: 0.92–11.12 mya) is not sufficiently precise to be dispositive of this putative causal scenario. The central mountain range uplifting was suggested as a barrier in the divergence of an aquatic subterranean arthropod, the stygobiont shrimp *Typhlocaris* Calman, 1909 (Guy-Haim et al., 2018). Guy-Haim et al. (2018) suggested a 7 mya divergence between *Typhlocaris galilea* Calman, 1909, found in a subterranean spring located at the Sea of Galilee seashore, and two Mediterranean *Typhlocaris* species: *T. ayyaloni* Tsurnamal, 2008 found in Ayyalon cave in Israel, and *T. salentina* Caroli, 1923 found in southern Italy (Guy-Haim et al., 2018; Tsurnamal, 2008).

Sarax ioanniticus is one of a handful of parthenogenetic species within Amblypygi, with a very small number of males reported from only two localities (Armas, 2000; Kovařík and Vlasta, 1996; Miranda et al. 2021a; Ribeirinho Vidal et al., 2021; Weygoldt, 2007). We infer that it likely represents a case of apomixis, wherein offspring are produced from unfertilized eggs that did not undergo meiosis (Simon et al., 2003). This type of thelytokous parthenogenesis results in a complete lack of genetic variation in both nuclear and mitochondrial genes among

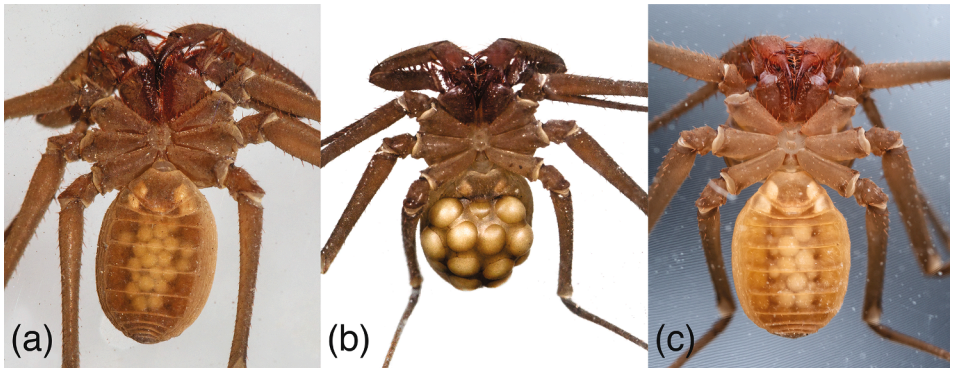

Fig. 4. Parthenogenesis in *S. israelensis*. (a) Adult female in ventral view several weeks after molting, showing developing oocytes. (b) Adult female carrying an egg clutch produced by parthenogenesis. (c) A subadult or small adult female in ventral view that was born in the laboratory and has been isolated since birth; note the developing oocytes visible in the ovary. Photos by G. Wizen.

Table 3
Natural history and rearing data for captive-bred specimens of *S. israelensis*.

Specimen no.	Locality	Date collected	Date molted	Date eggs	Date hatch	No. of offspring
1	Susita	8.v.2013	13.vii.2014	2.vii.2015	9.x.2015	13
2	Susita	21.vii.2013	25.viii.2014	7.vii.2015	1.x.2015	9
3	Susita	3.iv.2014	6.vi.2014	21.viii.2015	30.xi.2015	15
4	Susita	3.iv.2014	16.ii.2015	8.iv.2016	12.vii.2016	10
5	Susita	3.iv.2014	24.v.2015	20.ix.2016	26.xii.2016	17
6	Mimlach	3.iv.2014	18.xii.2014	7.xi.2015	8.ii.2016	15
7	Mimlach	3.iv.2014	20.xii.2014	13.xi.2015	16.ii.2016	25
8	Mimlach	4.iv.2015	27.vii.2015	30.viii.2016	1.xii.2016	14
9	Mimlach	4.iv.2015	16.xi.2015	29.ix.2016	31.xii.2016	21
10	Mimlach	4.iv.2015	20.xi.2015	25.ix.2016	20.xii.2016	17
11	Mimlach	7.vi.2015	4.i.2016	6.ix.2016	4.xii.2016	15

clones (as observed herein; Figs. 2, 3). This is additionally consistent with the near and complete absence, respectively, of males in *S. ioanniticus* and *S. israelensis* (a few males of *S. ioanniticus* have been reported from Turkey, see Miranda et al. 2021a). *Sarax ioanniticus* is known to be diploid, with 72 highly condensed chromosomes (Reyes Lerma et al., 2021). While the karyotype of *S. israelensis* has not been described, the next most closely related species, the sexually reproducing *S. seychellarum*, bears a complement of 22 chromosomes (Reyes Lerma et al., 2021). Due to the high variability of karyotype across the family (2n = 22–74), as well as the lack of flow cytometry data, it is unclear whether parthenogenesis in *S. ioanniticus* is attributable to an ancient polyploidization event, though this mechanism of parthenogenesis is thought to be rare even in arthropod groups that harbor relatively large proportions of parthenogens (e.g., haplodiploids) (van der Kooi et al., 2017). Problematically, however, apomictic parthenogenesis makes the evolutionary history and biogeography of the species difficult to infer. While the timing of the split between the species can be feasibly estimated, the lack of genetic variation within each species (due to clonal reproduction) renders molecular dating incapable of estimating the timing of colonization events within each species (Lorenzo-Carballa et al., 2012).

In some arthropod groups, parthenogenesis has been linked to higher dispersal ability and comparatively broader ecological niches in groups that otherwise exhibit low vagility. One classic example is the scorpion *Liocheles australasiae* (Fabricus 1775), which is widely distributed across both oceanic and continental islands in the western Pacific (Lourenço, 2000; Monod and Prendini, 2015) and has been shown to be able to stably maintain parthenogenesis for multiple generations in captivity (Makioka, 1993; Yamazaki and Makioka, 2005). Consistent with this pattern, *S. ioanniticus* exhibits a fairly large range for a single species of Amblypygi (Fig. 1), whereas many members of Charinidae exhibit single-terrane or even single-locality endemism (Giupponi and Miranda, 2016). Similar trends have been reported for other cases of parthenogenetic whip spiders, such as in the Caribbean (Armas, 2005). While future surveys of arachnid biodiversity are very likely to yield additional localities for *S. ioanniticus* across the Mediterranean region, it is unknown if *S. israelensis* is an endemic species to the north of Israel, or a more broadly distributed amblypygid. Yet, it is not clear why *S. israelensis* is geographically restricted to two sets of localities in Israel (with only one of these shared with *S. ioanniticus*). Competitive exclusion with respect to an older and more broadly distributed congener is a possible mechanism for the observed distributions, but the lack of genetic variance within both species makes this hypothesis difficult to test using molecular dating. Despite the sympatric occurrence of the two species in Mimlach cave, to our knowledge, no behavioral data exist with respect to interspecific antagonism or competition in this species pair.

The validation of parthenogenesis in *S. israelensis* using natural history data also suggests that variation in the degree of eye reduction may be entirely attributable to epigenetic mechanisms (e.g., differential methylation of coding regions) in this arachnid species. This phenomenon is contrary to the archetypal models of eye reduction and loss in other cave model species (e.g., *Astyanax* cavefish; cave isopods). However, our inference of phenotypic plasticity is consistent with previous observations of variance in the expression levels of retinal determination network transcription factors in genetically identical embryos of *S. israelensis*, and suggests that the degree of eye reduction may be even more plastic (i.e., environmentally determined) in cave arachnids than previously thought (Gainett et al., 2020).

The clear and unambiguous genetic break between *S. ioanniticus* and *S. israelensis*, together with the lack of variation within each species, renders the population dynamics of this pair fairly simple. Nevertheless, two peculiarities spring from the datasets generated for *S. israelensis*. First, there is the unusually large variation of median eye phenotype in *S. israelensis*, with some specimens exhibiting reduced (but clearly visible) ocelli, and others exhibiting virtual absence of eyes and eye

pigmentation (Fig. 3; Supplementary Fig. S1). For most cave-adapted species, such as *Astyanax*, these trends would be attributable to genetic variation in an incipient troglobite. However, *S. israelensis* exhibits genetic invariance and is likely a troglophile (like *S. ioanniticus*). The second peculiarity is the counterintuitive speciation process that gave rise to *S. ioanniticus* and *S. israelensis*. These two parthenogenetic whip spiders clearly constitute recently diverged sister taxa, with little genetic variance within each species. The most parsimonious reconstruction would therefore be a parthenogenetic ancestor that gave rise to two parthenogenetic daughter species. However, speciation after the transition to parthenogenesis is thought to be exceedingly rare, even in groups like haplodiploid insects that include large numbers of parthenogenetic species (Bell, 1982; Moreira et al., 2021; van der Kooi et al., 2017). Similarly, reversals to sexual reproduction from a parthenogenetic ancestor are understood to be rare events (van der Kooi and Schwander, 2014). The available sampling and sequence data for *S. ioanniticus* and *S. israelensis* instead support a less parsimonious scenario: both species constitute the result of a sexually reproducing ancestor that underwent speciation, followed by two independent transitions to parthenogenesis in the daughter species. This scenario accords best with the clear genetic break between the two species (an outcome that is not feasible if either *S. ioanniticus* or *S. israelensis* were the ancestral species; that is, if one species were nested inside the other). It also accords with the near-complete lack of genetic variance within each species (an outcome that disfavors a more complex scenario of transitions back to sexuality in the stem lineage of either species).

5. Conclusion

Despite our use of sophisticated molecular methods, we were unable to determine the biogeographic history of *S. israelensis*; due to the genetic invariance that stems from their parthenogenetic life history, there is simply no usable information in molecular sequence data that can inform the reconstruction of intraspecific history. We cannot say, for instance, whether Susita and Mimlach caves constitute relictual localities, i.e., the only places *S. israelensis* now inhabits after undergoing range contraction, or that Mimlach cave is part of a range expansion. It is also possible that these animals currently live in a broader area than presently appreciated, such as the *Milieu Souterrain Superficiel* (MSS), an underground network of cavities within rock fragments (Mammola et al., 2017, 2016). Future efforts to employ pitfall trapping in the MSS may therefore better clarify the life history of the species.

CRediT authorship contribution statement

Caitlin M. Baker: Investigation, Formal analysis, Writing – original draft. **Jesús A. Ballesteros:** Investigation, Formal analysis, Writing – review & editing. **Shlomi Aharon:** Investigation, Writing – review & editing. **Guilherme Gainett:** Investigation, Writing – review & editing. **Igor Armiach Steinpress:** Investigation, Writing – review & editing. **Gil Wizen:** Investigation, Writing – review & editing. **Prashant P. Sharma:** Investigation, Funding acquisition, Writing – original draft. **Efrat Gavish-Regev:** Investigation, Conceptualization, Supervision, Funding acquisition, Writing – review & editing.

Declaration of Competing Interest

The authors declare that they have no known competing financial interests or personal relationships that could have appeared to influence the work reported in this paper.

Acknowledgements

Specimens of Amblypygi were collected under permits 2013/40027, 2013/40085, 2014/40313, 2017/41718 and 2020/42450, issued to E. G.-R.; and permits 2012/38653, 2013/40027, 2014/40313, 2014/40503 and 2016/41370, issued to G.W. by the Israel National Parks Authority.

We thank A. Frumkin, B. Langford, E. Cohen (Israel Cave Research Center), and E. Levin for assistance with cave data and in the field. Sequencing was performed at the UW-Madison Biotechnology Center. Access to computing was provided by the Bioinformatics Resource Center (BRC) of the University of Wisconsin-Madison. Fieldwork in Israel was supported by a National Geographic Society Expeditions Council grant no. NGS-271R-18 to J.A.B.. This work is supported by the US-Israel Binational Science Foundation grant no. BSF-2019216 to P.P. S. and E.G.-R. This manuscript was improved by valuable comments from the associate editor Mike Rix, and from Miquel Arnedo and one anonymous reviewer.

Appendix A. Supplementary data

Supplementary data to this article can be found online at https://doi.org/10.1016/j.ympev.2022.107560.

References

Agapakis, G., Miranda, G.S., 2019. First record of *Charinus ioanniticus* (Arachnida, Amblypygi: Charinidae) from continental Europe. Arachnologische Mitteilungen: Arachnology Letters 58, 13. https://doi.org/10.30963/aramit5805.

Armas, L.F., 2005. Notas sobre la biología reproductiva del amblipígio partenogenético *Charinus acosta* (Quintero, 1983) (Amblypygi: Charinidae). Boletín de la Sociedad Entomológica Aragonesa 36.

Armas, L.F., 2000. Parthenogenesis in Amblypygi. Avicennia 12 (13), 133–134.

Barr, T.C., Holsinger, J.R., 1985. Speciation in Cave Faunas. Annu. Rev. Ecol. Syst. 16, 313–337. https://doi.org/10.1146/annurev.es.16.110185.001525.

Bell, G., 1982. The masterpiece of nature the evolution and genetics of sexuality. Croom Helm, London.

Besnier, F., Glover, K.A., 2013. ParallelStructure: A R Package to Distribute Parallel Runs of the Population Genetics Program STRUCTURE on Multi-Core Computers. PLoS ONE 8, e70651. https://doi.org/10.1371/journal.pone.0070651.

Bidegaray-Batista, L., Arnedo, M.A., 2011. Gone with the plate: the opening of the Western Mediterranean basin drove the diversification of ground-dweller spiders. BMC Evol Biol 11, 317. https://doi.org/10.1186/1471-2148-11-317.

Bouckaert, R., Heled, J., Kühnert, D., Vaughan, T., Wu, C.-H., Xie, D., Suchard, M.A., Rambaut, A., Drummond, A.J., 2014. BEAST 2: A Software Platform for Bayesian Evolutionary Analysis. PLoS Comput Biol 10, e1003537. https://doi.org/10.1371/journal.pcbi.1003537.

Bradic, M., Beerli, P., García-de León, F.J., Esquivel-Bobadilla, S., Borowsky, R.L., 2012. Gene flow and population structure in the Mexican blind cavefish complex (*Astyanax mexicanus*). BMC Evol Biol 12, 9. https://doi.org/10.1186/1471-2148-12-9.

Bradic, M., Teotónio, H., Borowsky, R.L., 2013. The population genomics of repeated evolution in the blind cavefish *Astyanax mexicanus*. Molecular Biology and Evolution 30, 2383–2400. https://doi.org/10.1093/molbev/mst136.

Castresana, J., 2000. Selection of Conserved Blocks from Multiple Alignments for Their Use in Phylogenetic Analysis. Molecular Biology and Evolution 17, 540–552. https://doi.org/10.1093/oxfordjournals.molbev.a026334.

Colla, A., Legittimo, C.M., Castellucci, F., Simeon, E., Miranda, G.S., 2020. First record of Amblypygi from Italy: *Charinus ioanniticus* (Charinidae). Arachnology 18. https://doi.org/10.13156/arac.2020.18.6.642.

Cope, E.D., 1896. The Primary Factors of Organic Evolution. Open Court Publishing, Chicago.

Dollo, L., 1893. Les lois de l'évolution. Bulletin de la Société Belge de Géologie de Paléontologie et d'Hydrologie 7, 164–166.

Earl, D.A., vonHoldt, B.M., 2011. STRUCTURE HARVESTER: a website and program for visualizing STRUCTURE output and implementing the Evanno method. Conservation Genet Resour 4, 359–361. https://doi.org/10.1007/s12686-011-9548-7.

Eaton, D.A.R., Overcast, I., 2020. ipyrad: Interactive assembly and analysis of RADseq datasets. Bioinformatics 36, 2592–2594. https://doi.org/10.1093/bioinformatics/btz966.

Edgar, R.C., 2004. MUSCLE: multiple sequence alignment with high accuracy and high throughput. Nucleic Acids Research 32, 1792–1797. https://doi.org/10.1093/nar/gkh340.

Esposito, L.A., Bloom, T., Caicedo-Quiroga, L., Alicea-Serrano, A.M., Sánchez-Ruíz, J.A., May-Collado, L.J., Binford, G.J., Agnarsson, I., 2015. Islands within islands: Diversification of tailless whip spiders (Amblypygi, *Phrynus*) in Caribbean caves. Molecular Phylogenetics and Evolution 93, 107–117. https://doi.org/10.1016/j.ympev.2015.07.005.

Evanno, G., Regnaut, S., Goudet, J., 2005. Detecting the number of clusters of individuals using the software structure: a simulation study. Mol Ecol 14, 2611–2620. https://doi.org/10.1111/j.1365-294X.2005.02553.x.

Gainett, G., Ballesteros, J.A., Kanzler, C.R., Zehms, J.T., Zern, J.M., Aharon, S., Gavish-Regev, E., Sharma, P.P., 2020. Systemic paralogy and function of retinal determination network homologs in arachnids. BMC Genomics 21, 811. https://doi.org/10.1186/s12864-020-07149-x.

de Giupponi, A.P., L., Miranda, G.S.,, 2016. Eight new species of *Charinus* Simon, 1892 (Arachnida: Amblypygi: Charinidae) endemic for the Brazilian Amazon, with notes on their conservational status. PLoS ONE 11, e0148277. https://doi.org/10.1371/journal.pone.0148277.

Gould, S.J., 1970. Dollo on Dollo's law: Irreversibility and the status of evolutionary laws. J Hist Biol 3, 189–212. https://doi.org/10.1007/BF00137351.

Guy-Haim, T., Simon-Blecher, N., Frumkin, A., Naaman, I., Achituv, Y., 2018. Multiple transgressions and slow evolution shape the phylogeographic pattern of the blind cave-dwelling shrimp *Typhlocaris*. PeerJ 6, e5268. https://doi.org/10.7717/peerj.5268.

Hoang, D.T., Chernomor, O., von Haeseler, A., Minh, B.Q., Vinh, L.S., 2018. UFBoot2: Improving the Ultrafast Bootstrap Approximation. Molecular Biology and Evolution 35, 518–522. https://doi.org/10.1093/molbev/msx281.

Howarth, F.G., 1993. High-Stress Subterranean Habitats and Evolutionary Change in Cave-Inhabiting Arthropods. The American Naturalist 142, S65–S77. https://doi.org/10.1086/285523.

Howarth, F.G., 1983. Ecology of Cave Arthropods. Annu. Rev. Entomol. 28, 365–389. https://doi.org/10.1146/annurev.en.28.010183.002053.

Howarth, F.G., 1980. The Zoogeography Of Specialized Cave Animals: A Bioclimatic Model. Evolution 34, 394–406. https://doi.org/10.1111/j.1558-5646.1980.tb04827.x.

Howarth, F.G., Moldovan, O.T., 2018. The Ecological Classification of Cave Animals and Their Adaptations, in: Moldovan, O.T., Kováč, Ľ., Halse, S. (Eds.), Cave Ecology, Ecological Studies. Springer International Publishing, Cham, pp. 41–67. https://doi.org/10.1007/978-3-319-98852-8_4.

Huxley, J.S., 1942. Evolution: The Modern Synthesis. Allen and Unwin, London.

Kalyaanamoorthy, S., Minh, B.Q., Wong, T.K.F., von Haeseler, A., Jermiin, L.S., 2017. ModelFinder: fast model selection for accurate phylogenetic estimates. Nat Methods 14, 587–589. https://doi.org/10.1038/nmeth.4285.

Katoh, K., Standley, D.M., 2013. MAFFT Multiple Sequence Alignment Software Version 7: Improvements in Performance and Usability. Molecular Biology and Evolution 30, 772–780. https://doi.org/10.1093/molbev/mst010.

Kovařík, F., Vlasta D., 1996. First report of Amblypygi (Charinidae: *Charinus ioanniticus*) from Turkey. Klapalekiana 32, 57–58.

Lorenzo-Carballa, M.O., Hadrys, H., Cordero-Rivera, A., Andrés, J.A., 2012. Population genetic structure of sexual and parthenogenetic damselflies inferred from mitochondrial and nuclear markers. Heredity 108, 386–395. https://doi.org/10.1038/hdy.2011.84.

Lourenço, W.R., 2000. Reproduction in scorpions, with special reference to parthenogenesis. In: European Arachnology. Aarhus University Press, Århus, pp. 71–85.

Makioka, T., 1993. Reproductive biology of the viviparous scorpion, *Liocheles australasiae* (Fabricius) (Arachnida, Scorpiones, Ischnuridae) IV. Pregnancy in females isolated from infancy, with notes on juvenile stage duration. Invertebrate Reproduction & Development 24, 207–211. https://doi.org/10.1080/07924259.1993.9672353.

Mammola, S., 2019. Finding answers in the dark: caves as models in ecology fifty years after Poulson and White. Ecography 42, 1331–1351. https://doi.org/10.1111/ecog.03905.

Mammola, S., Arnedo, M.A., Pantini, P., Piano, E., Chiappetta, N., Isaia, M., 2018a. Ecological speciation in darkness? Spatial niche partitioning in sibling subterranean spiders (Araneae : Linyphiidae : *Troglohyphantes*). Invert. Systematics 32, 1069. https://doi.org/10.1071/IS17090.

Mammola, S., Cardoso, P., Ribera, C., Pavlek, M., Isaia, M., 2018b. A synthesis on cave-dwelling spiders in Europe. J Zool Syst Evol Res 56, 301–316. https://doi.org/10.1111/jzs.12201.

Mammola, S., Giachino, P.M., Piano, E., Jones, A., Barberis, M., Badino, G., Isaia, M., 2016. Ecology and sampling techniques of an understudied subterranean habitat: the Milieu Souterrain Superficiel (MSS). Sci Nat 103, 88. https://doi.org/10.1007/s00114-016-1413-9.

Mammola, S., Goodacre, S.L., Isaia, M., 2018c. Climate change may drive cave spiders to extinction. Ecography 41, 233–243. https://doi.org/10.1111/ecog.02902.

Mammola, S., Isaia, M., 2017. Spiders in caves. Proc. R. Soc. B. 284, 20170193. https://doi.org/10.1098/rspb.2017.0193.

Mammola, S., Piano, E., Giachino, P.M., Isaia, M., 2017. An ecological survey of the invertebrate community at the epigean/hypogean interface. SB 24, 27–52. https://doi.org/10.3897/subtbiol.24.21585.

Matmon, A., Wdowinski, S., Hall, J.K., 2003. Morphological and structural relations in the Galilee extensional domain, northern Israel. Tectonophysics 371, 223–241. https://doi.org/10.1016/S0040-1951(03)00237-3.

Mayr, E., 1942. Systematics and the Origin of Species. Columbia University Press, New York.

Meirmans, P.G., Van Tienderen, P.H., 2004. genotype and genodive: two programs for the analysis of genetic diversity of asexual organisms. Mol Ecol Notes 4, 792–794. https://doi.org/10.1111/j.1471-8286.2004.00770.x.

Miranda, G.S., Aharon, S., Gavish-Regev, E., Giupponi, A.P.L., Wizen, G., 2016. A new species of *Charinus* Simon, 1892 (Arachnida: Amblypygi: Charinidae) from Israel and new records of *C. ioanniticus* (Kritscher, 1959). EJT 0. https://doi.org/10.5852/ejt.2016.234.

Miranda, G.S., Giupponi, A.P.L., Prendini, L., Scharff, N., 2021a. Systematic revision of the pantropical whip spider family Charinidae Quintero, 1986 (Arachnida, Amblypygi). EJT 772, 1–409. https://doi.org/10.5852/ejt.2021.772.1505.

Miranda, G.S., Giupponi, A.P.L., Scharff, N., Prendini, L., 2021b. Phylogeny and biogeography of the pantropical whip spider family Charinidae (Arachnida: Amblypygi). Zoological Journal of the Linnean Society 194, 136–180. https://doi.org/10.1093/zoolinnean/zlaa101.

Monod, L., Prendini, L., 2015. Evidence for Eurogondwana: the roles of dispersal, extinction and vicariance in the evolution and biogeography of Indo-Pacific Hormuridae (Scorpiones: Scorpionoidea). Cladistics 31, 71–111. https://doi.org/10.1111/cla.12067.

Mor, D., Michelson, H., Druckman, Y., Mimran, Y., Heimann, A., Goldberg, M., Sneh, A., 1997. Notes on the Geology of the Golan Heights: (based on the 1:50,000 Geological Maps of Har Odem and Qazrin Sheets by D. Mor and Gamla Sheet by H. Michelson and D. Mor). (No. GSI/15/97), Geological Survey of Israel. Israel Ministry of Natural Infrastructures, Jerusalem.

Moran, R.L., Jaggard, J.B., Roback, E.Y., Kenzior, A., Rohner, N., Kowalko, J.E., Ornelas-García, C.P., McGaugh, S.E., Keene, A.C., 2022. Hybridization underlies localized trait evolution in cavefish. iScience 25, 103778 https://doi.org/10.1016/j.isci.2022.103778.

Moreira, M.O., Fonseca, C., Rojas, D., 2021. Parthenogenesis is self-destructive for scaled reptiles. Biol. Lett. 17, rsbl.2021.0006, 20210006. https://doi.org/10.1098/rsbl.2021.0006.

Nguyen, L.-T., Schmidt, H.A., von Haeseler, A., Minh, B.Q., 2015. IQ-TREE: A Fast and Effective Stochastic Algorithm for Estimating Maximum-Likelihood Phylogenies. Molecular Biology and Evolution 32, 268–274. https://doi.org/10.1093/molbev/msu300.

Porras-Hurtado, L., Ruiz, Y., Santos, C., Phillips, C., Carracedo, Á., Lareu, M.V., 2013. An overview of STRUCTURE: applications, parameter settings, and supporting software. Front. Genet. 4 https://doi.org/10.3389/fgene.2013.00098.

Poulson, T.L., White, W.B., 1969. The Cave Environment. Science 165, 971–981. https://doi.org/10.1126/science.165.3897.971.

Prendini, L., Francke, O.F., Vignoli, V., 2010. Troglomorphism, trichobothriotaxy and typhlochactid phylogeny (Scorpiones, Chactoidea): more evidence that troglobitism is not an evolutionary dead-end. Cladistics 26, 117–142. https://doi.org/10.1111/j.1096-0031.2009.00277.x.

Pritchard, J.K., Stephens, M., Donnelly, P., 2000. Inference of Population Structure Using Multilocus Genotype Data. Genetics 155, 945–959. https://doi.org/10.1093/genetics/155.2.945.

Protas, M., Jeffery, W.R., 2012. Evolution and development in cave animals: from fish to crustaceans: Evolution and development in cave animals. WIREs Dev Biol 1, 823–845. https://doi.org/10.1002/wdev.61.

Protas, M.E., Hersey, C., Kochanek, D., Zhou, Y., Wilkens, H., Jeffery, W.R., Zon, L.I., Borowsky, R., Tabin, C.J., 2006. Genetic analysis of cavefish reveals molecular convergence in the evolution of albinism. Nat Genet 38, 107–111. https://doi.org/10.1038/ng1700.

Protas, M.E., Trontelj, P., Patel, N.H., 2011. Genetic basis of eye and pigment loss in the cave crustacean *Asellus aquaticus*. Proc. Natl. Acad. Sci. U.S.A. 108, 5702–5707. https://doi.org/10.1073/pnas.1013850108.

Rambaut, A., Drummond, A.J., Xie, D., Baele, G., Suchard, M.A., 2018. Posterior Summarization in Bayesian Phylogenetics Using Tracer 1.7. Systematic Biology 67, 901–904. https://doi.org/10.1093/sysbio/syy032.

Re, C., Fišer, Ž., Perez, J., Tacdol, A., Trontelj, P., Protas, M.E., 2018. Common genetic basis of eye and pigment loss in two distinct cave populations of the Isopod Crustacean *Asellus aquaticus*. Integrative and Comparative Biology 58, 421–430. https://doi.org/10.1093/icb/icy028.

Reyes Lerma, A.C., Šťáhlavský, F., Seiter, M., Carabajal Paladino, L.Z., Divišová, K., Forman, M., Sember, A., Král, J., 2021. Insights into the Karyotype Evolution of Charinidae, the Early-Diverging Clade of Whip Spiders (Arachnida: Amblypygi). Animals 11, 3233. https://doi.org/10.3390/ani11113233.

Ribeirinho Vidal, V.C., da Carvalho Filho, F., S., Silva de Miranda, G.,, 2021. Amblypygi parthenogenesis, embryonic and post-embryonic development: a case study with the Amazonian species *Charinus guto* Giupponi and Miranda, 2016 (Amblypygi: Charinidae). Journal of Natural History 55, 1113–1129. https://doi.org/10.1080/00222933.2021.1936678.

Riddle, M.R., Aspiras, A.C., Gaudenz, K., Peuß, R., Sung, J.Y., Martineau, B., Peavey, M., Box, A.C., Tabin, J.A., McGaugh, S., Borowsky, R., Tabin, C.J., Rohner, N., 2018. Insulin resistance in cavefish as an adaptation to a nutrient-limited environment. Nature 555, 647–651. https://doi.org/10.1038/nature26136.

Segev, A., Reznik, I.J., Schattner, U., 2022. Miocene to sub-Recent magmatism at the intersection between the Dead Sea Transform and the Ash Shaam volcanic field: evidence from the Yarmouk River gorge and vicinity. Geol. Mag. 159, 469–493. https://doi.org/10.1017/S0016756821001072.

Shakhatreh, M.R., Miranda, G.S., Bader-Katbeh, A., Abu Baker, M.A., Amr, Z.S., 2020. *Charinus ioanniticus* (Amblypygi: Charinidae), first record of a whip spider from Jordan. Arachnologische Mitteilungen: Arachnology Letters 59, 35. https://doi.org/10.30963/aramit5906.

Simon, J.-C., Delmotte, F., Rispe, C., Crease, T., 2003. Phylogenetic relationships between parthenogens and their sexual relatives: the possible routes to parthenogenesis in animals. Biological Journal of the Linnean Society 79, 151–163. https://doi.org/10.1046/j.1095-8312.2003.00175.x.

Tsurnamal,, 2008. A new species of the stygobiotic blind prawn Typhlocaris Calman, 1909 (Decapoda, Palaemonidae, Typhlocaridinae) from Israel. Crustac 81, 487–501. https://doi.org/10.1163/156854008783797534.

van der Kooi, C.J., Matthey-Doret, C., Schwander, T., 2017. Evolution and comparative ecology of parthenogenesis in haplodiploid arthropods. Evolution Letters 1, 304–316. https://doi.org/10.1002/evl3.30.

van der Kooi, C.J., Schwander, T., 2014. On the fate of sexual traits under asexuality: On the fate of sexual traits under asexuality. Biol Rev 89, 805–819. https://doi.org/10.1111/brv.12078.

Wagner, G.P., 1982. The logical structure of irreversible systems transformations: A theorem concerning Dollo's law and chaotic movement. Journal of Theoretical Biology 96, 337–346. https://doi.org/10.1016/0022-5193(82)90114-X.

Weygoldt, P., 2007. Parthenogenesis and Reproduction in *Charinus ioanniticus* (Kritscher, 1959) (Chelicerata, Amblypygi, Charinidae). Arachnology 14, 81–82. https://doi.org/10.13156/arac.2007.14.2.81.

Xia, X., 2018. DAMBE7: New and Improved Tools for Data Analysis in Molecular Biology and Evolution. Molecular Biology and Evolution 35, 1550–1552. https://doi.org/10.1093/molbev/msy073.

Yamazaki, K., Makioka, T., 2005. Parthenogenesis through five generations in the scorpion Liocheles australasiae (fabricius 1775) (Scorpiones, Ischnuridae). Journal of Arachnology 33, 852–856. https://doi.org/10.1636/S02-5.1.